

Quantum variational solving of the Wheeler-DeWitt equation

Grzegorz Czelusta and Jakub Mielczarek*

Institute of Theoretical Physics, Jagiellonian University, Lojasiewicza 11, 30-348 Cracow, Poland

One of the central difficulties in the quantization of the gravitational interactions is that they are described by a set of constraints. The standard strategy for dealing with the problem is the Dirac quantization procedure, which leads to the Wheeler-DeWitt equation. However, solutions to the equation are known only for specific symmetry-reduced systems, including models of quantum cosmology. Novel methods, which enable solving the equation for complex gravitational configurations are, therefore, worth seeking.

Here, we propose and investigate a new method of solving the Wheeler-DeWitt equation, which employs a variational quantum computing approach, possible to implement on quantum computers. For this purpose, the gravitational system is regularized, by performing spherical compactification of the phase space. This makes the system's Hilbert space finite-dimensional and allows to use $SU(2)$ variables, which are easy to handle in quantum computing. The validity of the method is examined in the case of the flat de Sitter universe. For the purpose of testing the method, both an emulator of a quantum computer and the IBM superconducting quantum computer have been used. Advantages and limitations of the approach are discussed.

I. INTRODUCTION

The Hamiltonian of General Relativity (GR) is a sum of constraints. The constraints are usually grouped into two sets: a single scalar (Hamiltonian) constraint S and a three-component vector constraint V , so that the gravitational Hamiltonian is:

$$H[N, \vec{N}] = S[N] + V[\vec{N}] = \int_{\Sigma} d^3x NC + \int_{\Sigma} d^3x \vec{N} \cdot \vec{C}, \quad (1)$$

where Σ is a spatial hypersurface. The N and \vec{N} are the lapse function and the shift vector respectively, which are integrated with the smeared constraints C and \vec{C} . By imposing the constraint on the kinematical phase space Γ_{kin} the physical phase space Γ_{phys} is obtained. However, due to the complicated form of the constraints (specifically the smeared scalar constraint C), extraction of the physical phase space is in general a difficult task.

This difficulty propagates onto the quantum case where the initial kinematical Hilbert space \mathcal{H}_{kin} is a subject of imposing the quantum constraints \hat{C} and $\hat{\vec{C}}$ in order to extract the physical states $|\Psi_{\text{phys}}\rangle$, belonging to the physical Hilbert space $\mathcal{H}_{\text{phys}} \subseteq \mathcal{H}_{\text{kin}}$ (the equality of sets $\mathcal{H}_{\text{phys}} = \mathcal{H}_{\text{kin}}$ corresponds to the trivial case of vanishing constraints). There are various strategies for approaching the problem.

Before we proceed to reviewing the most common of them let us restrict our considerations to the case of a single quantum constraint \hat{C} - the quantum Hamiltonian constraint (scalar constraint). This assumption is to simplify our considerations and make them more transparent. However, extension to the case of multiple constraints is, in principle, straightforward. Namely, a given

method of solving the single constraint has to be applied successively. However, additional technical difficulties may appear due to differences in the functional form of the constraints. Furthermore, the case with the single constraint \hat{C} corresponds to the case of homogenous minisuperspace models, which are relevant in (quantum) cosmology.

By extracting states which solve the quantum Hamiltonian constraint \hat{C} , a subspace \mathcal{H}_C of the kinematical Hilbert space \mathcal{H}_{kin} can be found. In general, the subspace \mathcal{H}_C , is further restricted by solving the quantum vector constraint $\hat{\vec{C}}$, leading to $\mathcal{H}_{\text{phys}}$, such that $\mathcal{H}_C \subseteq \mathcal{H}_{\text{phys}}$. However, in the special case of vanishing vector constraint (which is satisfied for certain minisuperspace models), we have $\mathcal{H}_C = \mathcal{H}_{\text{phys}}$. Therefore, in general, the following sequence of weak inclusions holds: $\mathcal{H}_{\text{phys}} \subseteq \mathcal{H}_C \subseteq \mathcal{H}_{\text{kin}}$, which is satisfied independently on whether the vector constraint is solved before or after the Hamiltonian constraint.

Perhaps the most common approach to determine \mathcal{H}_C is provided by the Dirac method of quantizing constrained systems. Here, taking the \hat{C} , which is a self-adjoint operator, one is looking for states which are annihilated by the operator, i.e.

$$\hat{C}|\Psi\rangle \approx 0, \quad (2)$$

where “ \approx ” denotes weak equality, i.e. satisfied for the states $|\Psi\rangle \in \mathcal{H}_C$. Eq. (2) is the famous Wheeler-DeWitt (WDW) equation. Solutions to the equation, which are belonging to the kernel of the operator \hat{C} , span the Hilbert space $\mathcal{H}_C = \ker \hat{C}$. The difficulty of the method lies in finding solution to the WDW equation. The solutions are known e.g. for certain quantum cosmological models [1, 2].

Extraction of the physical states can alternatively be performed employing the *group averaging* [3] approach, which utilizes the projection operator \hat{P} . The \hat{P} is a non-unitary, but self-adjoint ($\hat{P}^\dagger = \hat{P}$) and idempotent

* jakub.mielczarek@uj.edu.pl

($\hat{P}^2 = \hat{P}$) operator, which for the case of a constraint \hat{C} with a zero eigenvalue takes the following form:

$$\hat{P} = \lim_{T \rightarrow \infty} \frac{1}{2T} \int_{-T}^T d\tau e^{i\tau \hat{C}}. \quad (3)$$

The expression performs Dirac delta-like action on the kinematical states, projecting them onto the physical subspace.

Another widely explored method of finding the physical states is provided by the *reduced phase space* method [4], in which one looks for solution of the constraints already at the classical level. For gravity, this is perhaps not possible do in general. However, utility of the approach has been shown for certain minisuperspace models (see e.g. [5]). While the Γ_{phys} is extracted, the algebra of observables is a subject of quantization, leading to the physical Hilbert space $\mathcal{H}_{\text{phys}}$.

The method we are going to study here is based on the observation made in Ref. [6]. Namely, while a Hamiltonian constraint $C \approx 0$ is considered, the configurations satisfying the constraint can be found by identifying ground states of a new Hamiltonian C^2 . A possibility of extracting Γ_{phys} for a prototype classical constraint C with the use of adiabatic quantum computing has been discussed.

Here, we generalize the method to the quantum case and investigate its implementation on a universal quantum computer. The approach, utilizes Variational Quantum Eigensolver (VQE) [7], which is a hybrid quantum algorithm. The algorithm has been widely discussed in the literature, in particular in the context of quantum chemistry [8, 9]. While our VQE-based method is introduced in a general fashion, which does not depend on the particular form of \hat{C} , over the article we will mostly refer to the concrete case of \hat{C} , corresponding to a quantum cosmological model. The VQE will be implemented on both simulator of a quantum computer (employing Penny Lane [10] and Qiskit [11] tools) and on actual superconducting quantum computer provided by IBM [12].

Applying quantum computing methods unavoidably requires dealing with the finite systems - having finite dimensional Hilbert spaces. Because standard canonical quantization of gravitational system does not lead to finite dimensional Hilbert space representation, a procedure of cutting-off dimension of the Hilbert space has to be applied. For this purpose, we apply the recently introduced Non-linear Field Space Theory (NFST) [13], which provides a systematic procedure of compactifying phase spaces of the standard affine phase spaces. The compactification leads to finite volume of the phase space, and in consequence finite dimension of the Hilbert space. In case of the spherical compactification, of a \mathbb{R}^2 phase space, the control parameter of the cut-off is the total spin S , associated with the volume of the spherical phase space. In the large spin limit ($S \rightarrow \infty$), the standard case with an infinite dimensional Hilbert space is recovered. Depending on quantum computational resources, the value of S can be fixed such that the corresponding

Hilbert space can be represented with available number of logical qubits.

Additional advantage of the method introduced in the article is that finding physical states employing variational method gives as explicitly operator (i.e. ansatz with determined parameters) which can be used to generate the physical states on a quantum computer. The states can be used for further simulations on a quantum processor. For example, transitions amplitudes between the states can be evaluated. On the other hand, when the physical states are found using analytical methods or classical numerics, the difficulty of constructing operator preparing a given state remains.

The organization of the article is the following. In Sec. II, the method of regularizing the Hamiltonian constraint, employing compactification of the phase space is introduced. The procedure is applied to the case of de Sitter cosmology. Then, in Sec. III, general considerations concerning the VQE applied to solving the Hamiltonian constraint are made. The qubit representation of Hamiltonian constraint introduced in Sec. II is discussed in Sec. IV. In Sec. V the problem of determining fixed spin subspace of the physical Hilbert space is addressed. A quantum method of evaluating gradients in the VQE procedure is presented in Sec. VI. Examples of applying the procedure for the case of spin $s = 1$ is given in Sec. VII and in Sec. VIII for $s = 2$. The computational complexity considerations of the method are made in Sec. IX. The results are summarized in Sec. X.

II. COMPACT PHASE SPACE REGULARIZATION OF DE SITTER MODEL

The initial step towards quantum variational solving of the Wheeler-DeWitt equation is making system's Hilbert space finite. Actually, there are theoretical arguments for gravitational Hilbert space being locally finite [14]. Some of the approaches quantum gravity, aim to implement this property while performing quantization of gravitational degrees of freedom [15]. Here, we will follow a general procedure of making gravitational Hilbert space finite, which bases on compactification of the phase space. The approach is considered here as a particular, convenient way of performing regularization of quantum system. However, it may also play a role in formulating quantum theory of gravitational interaction. However, this second possibility is not explored here, and the method is used purely for technical reason.

A. Compact phase spaces

Let us recall that for a system with m classical degrees of freedom, dimension of the phase space Γ is $\dim\Gamma = 2m$. Having the symplectic form ω , defined at the phase space (which is a symplectic manifold), the volume of the space is $\mathcal{V} = \int_{\Gamma} \omega$. Following the Heisenberg uncertainty

principle one can now estimate the number of linearly independent vectors in the corresponding Hilbert space as:

$$\dim \mathcal{H} \sim \frac{\mathcal{V}}{(2\pi\hbar)^m}. \quad (4)$$

It should be noted that because the Heisenberg uncertainty may differ from the standard form while quantum gravitational degrees of freedom are considered, the formula (4) may be a subject of additional modifications. This should, however, not affect the general observation that dimension of the Hilbert space is monotonically dependent on the volume of the system's phase space. In consequence, finiteness of both the Hilbert space and the phase space are equivalent:

$$\dim \mathcal{H} < \infty \Leftrightarrow \mathcal{V} < \infty. \quad (5)$$

This allows us to conclude that by performing compactification of the phase space, the resulting quantum system will be characterized by a finite Hilbert space. The observation has been recently pushed forward in Non-linear Field Space Theory (NFST) [13], with the ambition of to introduce compact phase space generalizations not only of mechanical systems but also field theories. The procedure has been so far most extensively studied on the case of a scalar field.

For our purpose let us focus our attention on the case with finite number of classical degrees of freedom. This is in particular the situation of the so-called minisuperspace gravitational systems. Having the m classical degrees of freedom the standard symplectic form (in the Darboux basis) can be written as:

$$\omega = \sum_{i=1}^m \omega_i = \sum_{i=1}^m dp_i \wedge dq_i, \quad (6)$$

which is defined on the $\Gamma = \mathbb{R}^{2m}$ phase space. There are various ways of performing compactification of the phase space.

B. Spherical phase space

A simple and convenient approach is to replace every \mathbb{R}^2 subspace (corresponding to a given conjugated pair (q_i, p_i)) with a 2-sphere, \mathbb{S}^2 . So that, the total phase space, for the system having m classical degrees of freedom, becomes $\Gamma = \mathbb{S}^{2m}$. This replacement is possible because the \mathbb{S}^2 sphere is a symplectic manifold, and product of symplectic manifolds is also symplectic.

There are two main advantages of such a choice. First, is the fact that \mathbb{S}^2 is a phase space of angular momentum (spin) which results in easy to handle and well understood representation on both classical and quantum level. Second, a single new parameter S , associated with the volume of the phase space $\mathcal{V} = \int_{\mathbb{S}^2} \omega_{\mathbb{S}^2} = 4\pi S$, provides a natural control parameter of the regularization.

The flat (affine) limit is recovered by taking the $S \rightarrow \infty$ limit. On the other hand, selecting a given value of S precisely determines dimension of the Hilbert space. This is because quantization of the spherical phase space leads to condition $S = \hbar s$, where $s = \frac{n}{2}$, and $n \in \mathbb{N}$. For a given quantum number s , the associated Hilbert space \mathcal{H}_s has dimension $\dim \mathcal{H}_s = 2s + 1$, which leads to the concrete realization of the relation (4):

$$\dim \mathcal{H}_s = 2s + 1 = \frac{2S}{\hbar} + 1 = \frac{\mathcal{V}}{2\pi\hbar} + 1. \quad (7)$$

A natural symplectic form on the sphere is $\omega_{\mathbb{S}^2} = S \sin \theta d\phi \wedge d\theta$, where $\phi \in (-\pi, \pi]$ and $\theta \in [0, \pi]$ are spherical angles. It has been shown in [16] that by applying the change of variables $\varphi = \frac{p}{R_1}$ and $\theta = \frac{\pi}{2} + \frac{q}{R_2}$, together with condition $R_1 R_2 = S$, the symplectic form on the 2-sphere takes the form:

$$\omega = \cos \left(\frac{q}{R_2} \right) dp \wedge dq. \quad (8)$$

The symplectic form reduces to the flat case in the $S \rightarrow \infty$ ($R_{1,2} \rightarrow \infty$) limit. Therefore, the symplectic form (8) allows to recover the flat case as a local or the large S approximation (see Fig. 1).

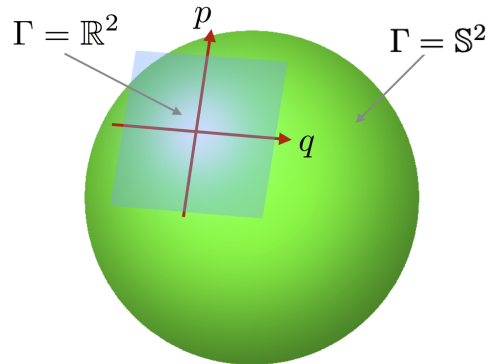


FIG. 1: Illustration of the spherical phase space and its local flat approximation.

Because the p and q variables do not provide a continuous parametrization of the sphere, it is convenient to work with the spin variables. Here, they correspond to the following Cartesian parametrization of the 2-sphere:

$$S_x = S \cos \left(\frac{p}{R_1} \right) \cos \left(\frac{q}{R_2} \right), \quad (9)$$

$$S_y = S \sin \left(\frac{p}{R_1} \right) \cos \left(\frac{q}{R_2} \right), \quad (10)$$

$$S_z = -S \sin \left(\frac{q}{R_2} \right), \quad (11)$$

together with the condition $S_x^2 + S_y^2 + S_z^2 = S^2$. Employing the symplectic form (8), which defines the Poisson bracket, one can verify that the spin components satisfy the $\mathfrak{su}(2)$ algebra $\{S_i, S_j\} = \epsilon_{ijk} S_k$, where $i, j, k \in$

$\{x, y, z\}$. The algebra is quantized in a straightforward manner, leading to the commutator algebra $[\hat{S}_i, \hat{S}_j] = i\hbar\epsilon_{ijk}\hat{S}_k$. Irreducible representations of the algebra are labeled by the spin s , such that:

$$\hat{S}^2|s, s_z\rangle = \hbar s(s+1)|s, s_z\rangle, \quad (12)$$

$$\hat{S}_z|s, s_z\rangle = \hbar s_z|s, s_z\rangle, \quad (13)$$

where $s_z = -s, -s+1, \dots, s_1, s$. The eigenstates $|s, s_z\rangle$ span the Hilbert space for a given representation, i.e. $\mathcal{H}_s = \text{span}\{|s, -s\rangle, \dots, |s, s\rangle\}$, and $\dim \mathcal{H}_s = 2s+1$. In what follows, for convenience, we set $\hbar = 1$.

Let us notice that the parametrization (9-11) is not a unique choice. In particular, in Ref. [17] polar parametrization of a spherical phase space was considered.

Having defined the spherical compactification procedure at the kinematical level, let us proceed to dynamics. The task is now to replace the flat space variables in constraints with the spin variables, valid for the spherical phase space. It has to be emphasized that the procedure is not unique. However, results of various assumptions, satisfying the correspondence to the flat phase space, should converge in the large S limit. A simple choice introduced in [16] is:

$$p \rightarrow \frac{S_y}{R_2} = R_1 \sin\left(\frac{p}{R_1}\right) \cos\left(\frac{q}{R_2}\right), \quad (14)$$

$$q \rightarrow -\frac{S_z}{R_1} = R_2 \sin\left(\frac{q}{R_2}\right), \quad (15)$$

so that the standard case is recovered in the $R_{1,2} \rightarrow \infty$ limit. For the system with N degrees of freedom, the same procedure is applied for each (q_i, p_i) pair.

C. de Sitter cosmological model

In this article, we will examine application of the compactification procedure to the flat de Sitter cosmological model. The gravitational Hamiltonian constraint for the model can be written as [16]:

$$C = q \left(-\frac{3}{4}\kappa p^2 + \frac{\Lambda}{\kappa} \right) \approx 0, \quad (16)$$

where $\kappa := 8\pi G$ and Λ is a positive cosmological constant. Here, the q and p form a canonical pair, for which the symplectic form is $\omega = dp \wedge dq$. The q is related with a cubed scale factor, so that, the Hubble factor is $H = \frac{1}{3}\frac{\dot{q}}{q}$. By solving the constraint, the Friedmann equation is obtained:

$$H^2 = \frac{\Lambda}{3}. \quad (17)$$

In Ref. [16] a compact phase space generalization of the flat de Sitter cosmological model has been introduced.

Following the procedure introduced in the previous subsection, one finds, that the compactified form of the constraint (16) is:

$$C = \frac{S_3}{R_1} \left[\frac{3}{4}\kappa \frac{S_2^2}{R_2^2} - \frac{\Lambda}{\kappa} \right], \quad (18)$$

where $R_1 R_2 = S$. By introducing the dimensionless parameter:

$$\delta := \frac{4}{3} \frac{\Lambda}{R_1^2 \kappa^2} \in [0, 1], \quad (19)$$

and by a proper rescaling, the constraint (18) can be rewritten into the form:

$$C \rightarrow \frac{4S^2}{3\kappa R_1} C = S_3 S_2^2 - \delta S^2 S_3. \quad (20)$$

Quantization of the constraint (20), which requires promoting of the phase space functions S_x, S_y and S_z into operators, and an appropriate symmetrization leads to:

$$\hat{C} = \frac{1}{3} \left(\hat{S}_z \hat{S}_y \hat{S}_y + \hat{S}_y \hat{S}_z \hat{S}_y + \hat{S}_y \hat{S}_y \hat{S}_z \right) - \delta \hat{S}^2 \hat{S}_z. \quad (21)$$

It has been shown in Ref. [16] that solutions to the WDW equation associated with the constraint (21) can be found. The solutions are, however, not in a direct form but are expressed in terms of the recursion equation. Furthermore, solutions to the WDW equation exist for the bosonic representations (integer s) and, in general, do not exist for the fermionic representations (half-integer s). The first non-trivial solution to the constraint (21) is for $s = 1$, for which the constraint takes the following matrix form:

$$\hat{C} = 2 \left(\frac{1}{6} - \delta \right) \begin{pmatrix} 1 & 0 & 0 \\ 0 & 0 & 0 \\ 0 & 0 & -1 \end{pmatrix} = 2 \left(\frac{1}{6} - \delta \right) \hat{S}_z. \quad (22)$$

The corresponding solution (excluding the trivial case of $\delta = \frac{1}{6}$) is given by the state:

$$|\Psi\rangle = \begin{pmatrix} 0 \\ 1 \\ 0 \end{pmatrix} = |s=1, s_z=0\rangle = \frac{1}{\sqrt{2}}(|01\rangle + |10\rangle), \quad (23)$$

where in the last equality, qubit representation of the state is given. Therefore, for $s = 1$, dimension of the kernel is $\dim \ker \hat{C} = 1$. On the other hand, as discussed in Ref. [16], for $s = 2$ dimension of the kernel depends on the value of δ . Namely, for $\delta \neq \frac{7}{18}$ we have $\dim \ker \hat{C} = 1$ and for $\delta = \frac{7}{18}$ we have $\dim \ker \hat{C} = 3$. Explicit form of the basis states spanning the kernels can be found in Ref. [16].

D. Qubit representation

The introduced compactification, not only leads to finite dimensional Hilbert space, but also is suitable for

simulations on a quantum computer. Expressing constraint with use of spin operators gives a natural qubit representation of the constraint. This is because, arbitrary spin s can be decomposed into spin-1/2 representations, which are qubits. One needs $n = 2s$ qubits to implement the spin s representation on a quantum register.

Moreover, eigenstates of spin operator exhibit symmetry, which can be used to simplify ansatz in variational methods. Eigenstates of the \hat{S}^2 operator are invariant under transformation changing order of qubits, i.e. for the operator $\hat{\mathcal{P}}$, defined as:

$$\hat{\mathcal{P}}|b_1 b_2 \dots b_n\rangle = |b_n b_{n-1} \dots b_1\rangle, \quad (24)$$

and if

$$\hat{S}^2|\psi\rangle = s(s+1)|\psi\rangle, \quad (25)$$

we have

$$\hat{\mathcal{P}}|\psi\rangle = |\psi\rangle. \quad (26)$$

One can simplify the variational ansatz by imposing the $\hat{\mathcal{P}}$ symmetry. Using variational methods we need to express our constraint in terms of unitary operators. These operators also exhibit the symmetry (i.e. $[\hat{C}, \hat{\mathcal{P}}] = 0$), so we can also reduce number of terms for which expectation value must be evaluated. Furthermore, utilizing gradient methods to minimize cost function we can use parameter shift rule, which can also be optimized according to the symmetry.

III. VARIATIONAL SOLVING OF A CONSTRAINT

Following the Dirac quantization method of constrained systems, our task is to determine the kernel of the operator \hat{C} . The kernel will correspond to the physical Hilbert space for the system $\mathcal{H}_{\text{phys}}$ and is spanned by the states $|\psi_0\rangle \in \mathcal{H}_{\text{phys}}$, annihilated by the Hamiltonian constraint, i.e. satisfying the WDW equation:

$$\hat{C}|\psi_0\rangle = 0. \quad (27)$$

For any linear operator \hat{C} , the above condition is equivalent to

$$\langle\psi_0|\hat{C}^\dagger\hat{C}|\psi_0\rangle = 0. \quad (28)$$

Moreover, one can prove that

$$\langle\psi|\hat{C}^\dagger\hat{C}|\psi\rangle \geq 0, \quad (29)$$

for all $|\psi\rangle$. In the case of self-adjoint operator \hat{C} , the corresponding conditions are:

$$\hat{C}|\psi_0\rangle = 0 \iff \langle\psi_0|\hat{C}^2|\psi_0\rangle = 0, \quad (30)$$

$$\langle\psi|\hat{C}^2|\psi\rangle \geq 0. \quad (31)$$

Following the Variational Quantum Eigensolver (VQE) methods, let us now assume that $|\psi(\boldsymbol{\alpha})\rangle$ is a state parameterized by a vector $\boldsymbol{\alpha} = \{\alpha_i\}_{i=1,\dots,p}$. In order to find $|\psi_0\rangle$ we have to find a minimum of non-negative cost function $c(\boldsymbol{\alpha})$, which is defined as follow:

$$c(\boldsymbol{\alpha}) := \langle\psi(\boldsymbol{\alpha})|\hat{C}^\dagger\hat{C}|\psi(\boldsymbol{\alpha})\rangle. \quad (32)$$

In case of self-adjoint operator \hat{C} , the cost function takes the form:

$$c(\boldsymbol{\alpha}) = \langle\psi(\boldsymbol{\alpha})|\hat{C}^2|\psi(\boldsymbol{\alpha})\rangle. \quad (33)$$

To find minimum of c we use some classical minimizing algorithm (on classical computer) but the value of c , i.e. expectation value of $\hat{C}^\dagger\hat{C}$ is computed using a quantum computer. The algorithm is initialized with some random parameters $\boldsymbol{\alpha}_0$. Then, by evaluating the quantum circuit, we obtain $c(\boldsymbol{\alpha}_i)$ and using classical algorithm we find new parameters $\boldsymbol{\alpha}_{i+1}$, which are closer to minimum, we repeat this steps (see Fig. 2). Eventually, the set of values:

$$\boldsymbol{\alpha}_{\min} := \arg \min_{\boldsymbol{\alpha}} c(\boldsymbol{\alpha}) \quad (34)$$

is found, such that:

$$|\psi_0\rangle = |\psi(\boldsymbol{\alpha}_{\min})\rangle. \quad (35)$$

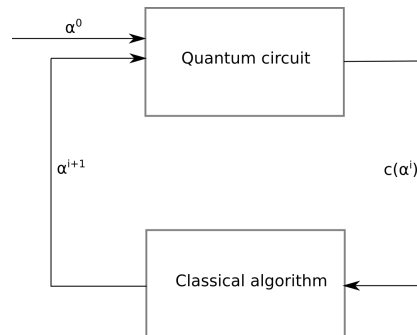


FIG. 2: Schematic illustration of the algorithm of finding minimum of cost function, evaluated by a quantum circuit.

Because, in general, the kernel space is more than one dimensional, there are different $|\psi_0\rangle$, which satisfy the condition (34). From the perspective of the operator $\hat{C}^\dagger\hat{C}$, this reflects the fact that its ground state is degenerated. Therefore, the algorithm must be designed such that the whole degeneracy space is sampled.

There are basically two main methods of evaluating the cost function of a quantum computer. The first approach utilizes the so-called Hadamard Test and the second follows the method discussed in Ref. [18].

Expectation value of any unitary operator \hat{U} in state $|\psi\rangle$ can be measured using Hadamard Test (Fig. 3), where

$$\hat{V}_\psi|0\rangle = |\psi\rangle. \quad (36)$$

The expectation value of \hat{U} is equal to the expectation value of the operator $2\sigma_+ = \sigma_x + i\sigma_y$ on the first qubit. When \hat{U} is self-adjoint and gives only real expectation values we can measure just $\langle\sigma_x\rangle$.

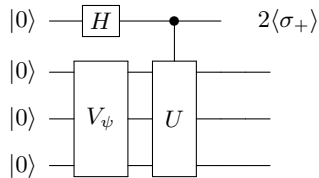


FIG. 3: The Hadamard test - a circuit measuring expectation value of \hat{U} in state $|\psi\rangle$.

In order to compute $\langle 2\sigma_+ \rangle = \langle\sigma_x\rangle + i\langle\sigma_y\rangle$ we need to compute $\langle\sigma_x\rangle$ and $\langle\sigma_y\rangle$. First, we need to apply gate which allows rotating base from computational one to base of eigenvectors of given operator. In the case of $\langle\sigma_x\rangle$, we need to apply Hadamard operator \hat{H} and take a measurement of σ_z in the computational bases, then

$$\langle\sigma_x\rangle = \langle\hat{H}\sigma_z\hat{H}\rangle = P(0) - P(1). \quad (37)$$

In the case of $\langle\sigma_y\rangle$, we need to apply operator $\hat{H}\hat{S}^\dagger$, where $\hat{S} = \begin{pmatrix} 1 & 0 \\ 0 & i \end{pmatrix}$ and take a measurement of σ_z in the computational bases, then

$$\langle\sigma_y\rangle = \langle\hat{S}\hat{H}\sigma_z\hat{H}\hat{S}^\dagger\rangle = P(0) - P(1). \quad (38)$$

The another method of evaluating expectation value of a unitary operator without additional qubit utilizes the the following formula:

$$\langle\psi|\hat{U}|\psi\rangle = \langle 0|\hat{V}_\psi^\dagger\hat{U}\hat{V}_\psi|0\rangle. \quad (39)$$

So, when we apply the operators V_ψ , U , V_ψ^\dagger on the initial state $|0\rangle$, and measure probability of a state $|0\rangle$ in the final state we obtain $|\langle\psi|\hat{U}|\psi\rangle|^2$ (see Fig. 4).

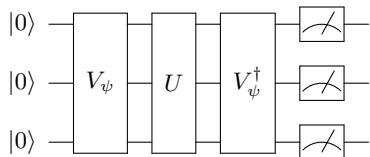


FIG. 4: Circuit measuring expectation value of \hat{U} in state $|\psi\rangle$.

In both methods, the \hat{U} is a unitary operator. In the case of non-unitary operators one has to express the operator as a sum of unitary operators and compute expectation value of each unitary term separately.

IV. COMPUTING EXPECTATION VALUES

Let us now proceed to the implementation of the algorithm introduced in the previous section. For this purpose, a method of evaluating the mean value of the operator \hat{C}^2 has to be introduced.

Our strategy is to express \hat{C} as sum of tensor products of Pauli operators (for the spin-1/2 representation):

$$\hat{C} = \sum_j c_j \bigotimes_i \hat{\sigma}_{ij}^k \quad (40)$$

where $k = x, y, z$ indicates one of the Pauli matrices, i is a index of a qubit and j is a index of a term in the sum. The c_j are constants multiplying given product of Pauli operators contributing to the sum. Then each part of this sum is an unitary operator and expectation value can be easily calculated

$$\langle\hat{C}\rangle = \sum_j c_j \langle\bigotimes_i \hat{\sigma}_{ij}^k\rangle. \quad (41)$$

Here, we apply the method to the constraint (21), which is a function of the spin variables \hat{S}_i , corresponding to a spin number s . The operators can be expressed in term of the Pauli matrices as follows:

$$\hat{S}_i = \frac{1}{2} \sum_{j=1}^n \mathbb{I}^1 \otimes \dots \mathbb{I}^{j-1} \otimes \hat{\sigma}_i^j \otimes \mathbb{I}^{j+1} \otimes \dots \mathbb{I}^n, \quad (42)$$

where $n = 2s$. It is easy to verify, that the spin components \hat{S}_i obey the commutation relation:

$$\begin{aligned} [\hat{S}_i, \hat{S}_j] &= \left[\frac{1}{2} \sum_m \hat{\sigma}_i^m, \frac{1}{2} \sum_n \hat{\sigma}_j^n \right] = \frac{1}{4} \sum_{m,n} [\hat{\sigma}_i^m, \hat{\sigma}_j^n] \\ &= \frac{1}{4} \sum_n [\hat{\sigma}_i^n, \hat{\sigma}_j^n] = \frac{1}{2} \sum_n i\epsilon_{ijk} \hat{\sigma}_k^n \\ &= i\epsilon_{ijk} \hat{S}_k, \end{aligned} \quad (43)$$

$$(44)$$

where the condition

$$[\hat{\sigma}_i^m, \hat{\sigma}_j^n] = 0 \quad (45)$$

for $m \neq n$ has been used. For convenience, we also define:

$$P_n(\sigma_i) := \sum_j \mathbb{I}^1 \otimes \dots \mathbb{I}^{j-1} \otimes \sigma_i^j \otimes \mathbb{I}^{j+1} \otimes \dots \mathbb{I}^n, \quad (46)$$

$$P_n(\sigma_i, \sigma_j) := \sum_{k,l,k \neq l} \mathbb{I}^1 \otimes \dots \mathbb{I}^{k-1} \otimes \sigma_i^k \otimes \mathbb{I}^{k+1} \otimes \dots \mathbb{I}^{l-1} \otimes \sigma_j^l \otimes \mathbb{I}^{l+1} \otimes \dots \mathbb{I}^n, \quad (47)$$

$$P_n(\sigma_i, \sigma_j, \sigma_p) := \sum_{k,l,q,k \neq l, k \neq q, l \neq q} \mathbb{I}^1 \otimes \dots \sigma_i^k \otimes \dots \sigma_j^l \otimes \dots \sigma_p^q \otimes \dots \mathbb{I}^n, \quad (48)$$

so that we can express

$$\hat{S}_i = \frac{1}{2} P_n(\sigma_i), \quad (49)$$

$$\hat{S}_i \hat{S}_j = \frac{1}{4} (P_n(\sigma_i, \sigma_j) + i\epsilon_{ijk} P_n(\sigma_k) + n\delta_{ij} \mathbb{I}^{\otimes n}), \quad (50)$$

$$\begin{aligned} 8\hat{S}_i \hat{S}_j \hat{S}_l &= P_n(\sigma_i, \sigma_j, \sigma_l) + i\epsilon_{ilk} P_n(\sigma_k, \sigma_j) \\ &\quad + i\epsilon_{jlk} P_n(\sigma_k, \sigma_i) + i\epsilon_{ijk} P_n(\sigma_k, \sigma_l) \\ &\quad + \delta_{il} (n-1) P_n(\sigma_j) + \delta_{jl} (n-1) P_n(\sigma_i) \\ &\quad - \epsilon_{ijk} \epsilon_{klm} P_n(\sigma_m) + \delta_{ij} n P_n(\sigma_l) + i\epsilon_{ijl} n \mathbb{I}^{\otimes n}. \end{aligned} \quad (51)$$

Applying these expressions to Eq. 21, we find that:

$$\begin{aligned} \hat{C} &= \frac{1}{8} \left((1-\delta) P_n(\sigma_z, \sigma_y, \sigma_y) - \delta P_n(\sigma_z, \sigma_x, \sigma_x) \right. \\ &\quad \left. - \delta P_n(\sigma_z, \sigma_z, \sigma_z) + \left(n - \frac{2}{3} - \delta(5n-2) \right) P_n(\sigma_z) \right). \end{aligned} \quad (52)$$

For the purpose of constructing the cost function, square of the operator \hat{C} has to be evaluated. Employing methods of symbolic algebra, the expression for \hat{C}^2 can be found explicitly:

$$\begin{aligned}
\hat{C}^2 = & \frac{1}{64} \left(P_n(\sigma_y, \sigma_y, \sigma_y, \sigma_y, \sigma_z, \sigma_z) (1-\delta)^2 + P_n(\sigma_y, \sigma_y, \sigma_y, \sigma_y) (n-4) (1-\delta)^2 \right. \\
& + P_n(\sigma_y, \sigma_y, \sigma_z, \sigma_z) \left(4(n-4) (1-\delta)^2 - 8\delta(1-\delta) - 6(n-4)\delta(1-\delta) - 12\delta^2 + 2 \left(\frac{3n-2}{3} - \delta(5n-2) \right) (1-\delta) \right) \\
& + P_n(\sigma_y, \sigma_y) \left(4(n-2)(n-3) (1-\delta)^2 - 8(n-2)\delta^2 + 2(n-2) \left(\frac{3n-2}{3} - \delta(5n-2) \right) (1-\delta) \right) \\
& + P_n(\sigma_z, \sigma_z) \left(2(n-2)(n-3) (1-\delta)^2 + 20(n-2)(n-3)\delta^2 + \left(\frac{3n-2}{3} - \delta(5n-2) \right)^2 \right. \\
& \left. + 4(n-2)\delta(1-\delta) - 6(n-2) \left(\frac{3n-2}{3} - \delta(5n-2) \right) \delta \right) \\
& + \mathbb{I}^{\otimes n} \left(2n(n-1)(n-2) (1-\delta)^2 + 8n(n-1)(n-2)\delta^2 + n \left(\frac{3n-2}{3} - \delta(5n-2) \right)^2 \right) \\
& + P_n(\sigma_x, \sigma_x) \left(4(n-2) (1-\delta)^2 + 4(n-2)(n-3)\delta^2 + 12(n-2)\delta(1-\delta) - 2(n-2) \left(\frac{3n-2}{3} - \delta(5n-2) \right) \delta \right) \\
& + P_n(\sigma_x, \sigma_x, \sigma_x, \sigma_x, \sigma_z, \sigma_z) \delta^2 + P_n(\sigma_x, \sigma_x, \sigma_x, \sigma_x) (n-4)\delta^2 \\
& + P_n(\sigma_x, \sigma_x, \sigma_z, \sigma_z) \left(10(n-4)\delta^2 - 8\delta(1-\delta) - 2 \left(\frac{3n-2}{3} - \delta(5n-2) \right) \delta + 12\delta(1-\delta) \right) \\
& + P_n(\sigma_z, \sigma_z, \sigma_z, \sigma_z, \sigma_z, \sigma_z) \delta^2 - 2P_n(\sigma_x, \sigma_x, \sigma_y, \sigma_y, \sigma_z, \sigma_z) \delta(1-\delta) \\
& + P_n(\sigma_z, \sigma_z, \sigma_z, \sigma_z) \left(9(n-4)\delta^2 - 2 \left(\frac{3n-2}{3} - \delta(5n-2) \right) \delta + 4\delta(1-\delta) \right) \\
& + P_n(\sigma_x, \sigma_x, \sigma_y, \sigma_y) \left(-2\delta(1-\delta)(n-4) + 2(1-\delta)^2 + 4\delta^2 + 8\delta(1-\delta) \right) \\
& \left. - 2P_n(\sigma_y, \sigma_y, \sigma_z, \sigma_z, \sigma_z, \sigma_z) \delta(1-\delta) + 2P_n(\sigma_x, \sigma_x, \sigma_z, \sigma_z, \sigma_z, \sigma_z) \delta^2 \right). \tag{53}
\end{aligned}$$

V. FIXED SPIN SUBSPACE OF A QUANTUM REGISTER

In order to find the kernel of \hat{C} we have to generate states $|\psi(\boldsymbol{\alpha})\rangle$. In case of 2 qubits we can use circuits allowing to generate any state, but in case of the arbitrary many qubits there are no such algorithms and we have to use some ansatz, for example R_y or $R_y R_z$ ansatz. Furthermore, often we want to look for the states only in some subspace of all possible n -qubits states. This is the case in the model under consideration for which the constraint (21) is defined in the spin- s subspace of the quantum register of n -qubits. One possible approach to this issue is generating only states obeying a given condition. The possibility is, however, difficult to implement in general. Another solution is to generate arbitrary states of the n -qubit register and adding a second term to the cost function, which fixes a given spin- s subspace.

Let us consider selection of a subspace, which is an eigenspace of some operator \hat{D} :

$$\hat{D}|\psi_d\rangle = d|\psi_d\rangle. \tag{54}$$

Then, we have to extend the cost function by adding a

term which has minimum value (equal 0) for states from this subspace, i.e.

$$\begin{aligned}
& \langle \psi | \left(\hat{D} - d\mathbb{I} \right)^\dagger \left(\hat{D} - d\mathbb{I} \right) | \psi \rangle \\
& = \langle \hat{D}^\dagger \hat{D} \rangle_\psi - 2\Re \left(d \langle \hat{D}^\dagger \rangle_\psi \right) + |d|^2. \tag{55}
\end{aligned}$$

In consequence, the new cost function takes form:

$$\begin{aligned}
c(\boldsymbol{\alpha}) = & \langle \psi(\boldsymbol{\alpha}) | \hat{C}^\dagger \hat{C} | \psi(\boldsymbol{\alpha}) \rangle \\
& + \langle \psi(\boldsymbol{\alpha}) | \left(\hat{D} - d\mathbb{I} \right)^\dagger \left(\hat{D} - d\mathbb{I} \right) | \psi(\boldsymbol{\alpha}) \rangle. \tag{56}
\end{aligned}$$

Due to the numerical minimization issues it is, however, better to consider a normalized cost function. In our case, we normalized both terms individually, so the normalized first term is equal:

$$\frac{1}{\max |\lambda_i|^2} \langle \psi(\boldsymbol{\alpha}) | \hat{C}^\dagger \hat{C} | \psi(\boldsymbol{\alpha}) \rangle \tag{57}$$

where $\max |\lambda_i|^2$ is the modulus square of the biggest

eigenvalue of \hat{C} . The normalized second term is equal:

$$\frac{1}{\max |d_i - d|^2} \langle \psi(\boldsymbol{\alpha}) | (\hat{D} - d\mathbb{I})^\dagger (\hat{D} - d\mathbb{I}) | \psi(\boldsymbol{\alpha}) \rangle, \quad (58)$$

where d_i are eigenvalues of \hat{D} .

In case we do not know these eigenvalues *a priori* we can treat them as some parameter that has to be adjusted during simulation or we can try to maximize the cost function and in this way estimate the value of $\max |\lambda_i|^2$. At the end, we normalize both terms dividing them by 2 (we also can take these two terms with some different weights than $\frac{1}{2}$ in order to improve performance of algorithms in some cases). In this way, the cost function takes values from the interval $[0, 1]$:

$$0 \leq c(\boldsymbol{\alpha}) \leq 1. \quad (59)$$

In case of the constraint (21), we want to look for a kernel in subspace of a given spin s . Therefore, we need to take cost function with $\hat{D} = \hat{S}^2 = \hat{D}^\dagger$ and $d = s(s+1)$. However, in this case we can choose simpler second term of cost function:

$$s(s+1) - \langle \hat{S}^2 \rangle, \quad (60)$$

which after normalization is:

$$1 - \frac{\langle \hat{S}^2 \rangle}{s(s+1)}. \quad (61)$$

Because (assuming that we use only $n = 2s$ qubits) the operator \hat{S}^2 has maximal expectation value equal to $s(s+1)$ and minimal equal 0, so

$$0 \leq 1 - \frac{\langle \hat{S}^2 \rangle}{s(s+1)} \leq 1. \quad (62)$$

The 0 value corresponds only to the states with spin s . So the whole cost function has zero value only for states which are simultaneously in the kernel of \hat{C} and have spin s . As a spin operator can be expressed in terms of qubits, employing Eq. 49, we find that:

$$\begin{aligned} \hat{S}^2 &= \sum_{i=x,y,z} S_i^2 = \frac{3}{4} n \mathbb{I}^{\otimes n} + \frac{1}{4} P_n(\sigma_x, \sigma_x) \\ &+ \frac{1}{4} P_n(\sigma_y, \sigma_y) + \frac{1}{4} P_n(\sigma_z, \sigma_z), \end{aligned} \quad (63)$$

and consequently:

$$\begin{aligned} \langle \hat{S}^2 \rangle &= \frac{3}{4} n + \frac{1}{4} \langle P_n(\sigma_x, \sigma_x) \rangle \\ &+ \frac{1}{4} \langle P_n(\sigma_y, \sigma_y) \rangle + \frac{1}{4} \langle P_n(\sigma_z, \sigma_z) \rangle. \end{aligned} \quad (64)$$

A. Degenerate kernel

In the case of degenerate kernel (i.e. there are more than one eigenstates for eigenvalue 0) we have to first find some eigenstate $|\psi_1\rangle$ using presented cost function and then in order to find another eigenstate (orthogonal to first one) we have to add to the cost function following term:

$$|\langle \psi_1 | \psi(\boldsymbol{\alpha}) \rangle|. \quad (65)$$

This term can easily be evaluated using $\langle 0 | \hat{V}_{\psi_1} \hat{V}_{\psi(\boldsymbol{\alpha})}^\dagger | 0 \rangle$, where \hat{V}_ψ generates state $|\psi\rangle$. Using this new cost function we can find another state from kernel $|\psi_2\rangle$ and then, adding to cost function new term

$$|\langle \psi_2 | \psi(\boldsymbol{\alpha}) \rangle|, \quad (66)$$

we can find the third state, and so on.

Another method is to find different vectors from kernel using algorithm starting from different initial parameters and then orthogonalize these vectors using the Gram-Schmidt procedure. When Gram-Schmidt returns zero vector that means that we reached dimension of the kernel (or that we generated linearly dependent vector so we have to repeat procedure to have high level of confidence that there are no more linearly independent vectors in kernel subspace).

VI. GRADIENT METHODS

In order to find minimum of cost function one needs to use some classical optimizer. There are possible choices of optimizers which do not need gradient of cost function, for example, COBYLA optimizer [19]. But one can get better performance using gradient descent optimizer, for example a basic gradient descent optimizer which in each step computes the new values according to the rule:

$$x^{(t+1)} = x^{(t)} - \eta \nabla f(x^{(t)}). \quad (67)$$

Another possibility are some more sophisticated algorithms like the Adam optimizer [20]. Using gradient method one needs to compute gradient of a cost function. One way to do so is to calculate values of the cost function in two points and compute numerical derivative by a finite differences. Another way is to use the parameter-shift rule [21]. Let us consider function f , which is an expectation value of some operator \hat{U} in some, parametrized by θ , state $|\psi(\theta)\rangle = \hat{V}_\theta |0\rangle$:

$$f(\theta) = \langle U \rangle_{\psi_\theta} = \langle 0 | V_\theta^\dagger U V_\theta | 0 \rangle \quad (68)$$

and assume that V_θ can be factorized (i.e. in circuit representing V_θ there is one-qubit gate G_{θ_i}):

$$V_\theta = A_{\theta_0, \dots, \theta_{i-1}} G_{\theta_i} B_{\theta_{i+1}, \dots, \theta_n} \quad (69)$$

where

$$G_{\theta_i} = e^{-i\theta_i \mathcal{G}}, \quad (70)$$

and \mathcal{G} is a self-adjoint operator with two different eigenvalues $-r, +r$. Then, exact (not approximate) derivative of f with respect to θ_i is:

$$\partial_{\theta_i} f = r(f(\theta_i + s) - f(\theta_i - s)) \quad (71)$$

where $s = \frac{\pi}{4r}$. In frequent cases of rotations around Pauli matrices (as in popular ansatzs): $G = R_y, R_x, R_z$, parameter r equals 1. Computation of difference between shifted functions can be made in one circuit using ancilla qubit and by controlling G gate (see Fig. 5). Then, the expectation value of $2\langle\sigma_+\rangle$ is equal to derivative of f :

$$2\langle\sigma_+\rangle = f(\theta_i + s) - f(\theta_i - s) = \partial_{\theta_i} f. \quad (72)$$

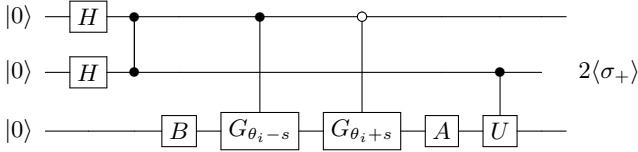


FIG. 5: Parameter-shift rule in the case of one-qubit states and operators.

VII. THE $s = 1$ CASE

As the first example of the introduced method, let us consider the special case of $s = 1$, for which the constraint takes form:

$$\hat{C} = \left(\frac{1}{6} - \delta\right) P_n(\sigma_z) = \left(\frac{1}{6} - \delta\right) (\sigma_z \otimes \mathbb{I} + \mathbb{I} \otimes \sigma_z), \quad (73)$$

and its square

$$\hat{C}^2 = 2 \left(\frac{1}{6} - \delta\right)^2 (\mathbb{I} \otimes \mathbb{I} + \sigma_z \otimes \sigma_z). \quad (74)$$

Therefore, we need to compute only one expectation value:

$$\langle\hat{C}^2\rangle = 2 \left(\frac{1}{6} - \delta\right)^2 (1 + \langle\sigma_z \otimes \sigma_z\rangle). \quad (75)$$

The quantum circuit enabling measuring the expectation value $\langle\sigma_z \otimes \sigma_z\rangle$ is shown in Fig. 6.

As the \hat{V}_ψ operator we use the RYCZ ansatz with two angles $\theta_1, \theta_2 \in [0, 2\pi)$ (see Appendix A). The quantum circuit for the ansatz is shown in Fig. 7. We reduced number of parameters from 4 to 2 using symmetry of our constraint, which induces symmetry of states from the kernel. The states are, namely, invariant under changing qubits order from q_1, q_2, \dots, q_n to q_n, q_{n-1}, \dots, q_1 .

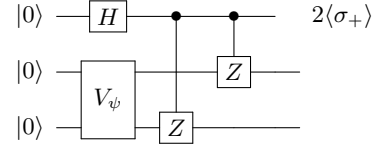


FIG. 6: Circuit measuring expectation value $\langle\sigma_z \otimes \sigma_z\rangle$ in state $|\psi\rangle$.

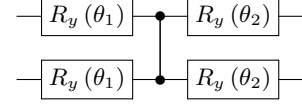


FIG. 7: Quantum circuit for the ansatz for spin 1.

In this example, basic gradient-descent optimizer was used with stepsize $\eta = 1$ and convergence tolerance was 10^{-6} . Parameter δ in constraint was set to $\frac{1}{2}$.

Fig. 8 shows the cost function in a function of steps of the optimization procedure.

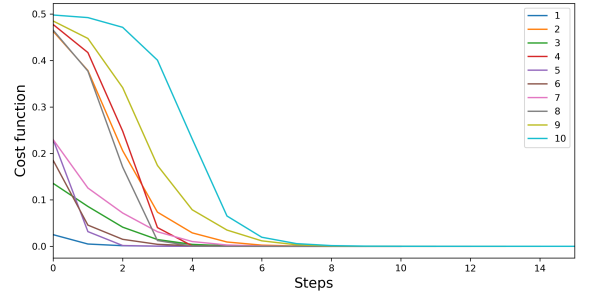


FIG. 8: Cost function during minimalization for 10 runs with randomly initialize parameters.

Fig. 9 shows cost function in the parameter space. We see four minima, each corresponds to the same state (up to a global phase). It is worth noticing that the landscape of the cost function does not possess any local minima, which simplifies the optimization procedure. This, however, not necessarily the case for higher spins, including the spin 2 example discussed in the next section.

Obtained amplitudes of the basis states are shown on Fig. 13. The algorithm returns correct states up to global phase ± 1 , on plot signs are agreed. The states are very close to exact result, which is a state $\frac{1}{\sqrt{2}}(|01\rangle + |10\rangle)$ (see Eq. 23), with quantum fidelity equal 1, up to numerical uncertainty. Because the RYCZ ansatz corresponds to a pure state, the quantum fidelity reduces to $F(\hat{\rho}_1, \hat{\rho}_2) = |\langle\psi_1|\psi_2\rangle|^2$, where $\hat{\rho}_1 = |\psi_1\rangle\langle\psi_1|$ and $\hat{\rho}_2 = |\psi_2\rangle\langle\psi_2|$.

For this simple case we also made computation on real IBM superconducting quantum processor Yorktown [12]. The quantum processor has topology of qubits shown on Fig. 10. In the simulations, 1024 of shots for each circuit has been made.

Fig. 11 shows the cost function in a function of steps

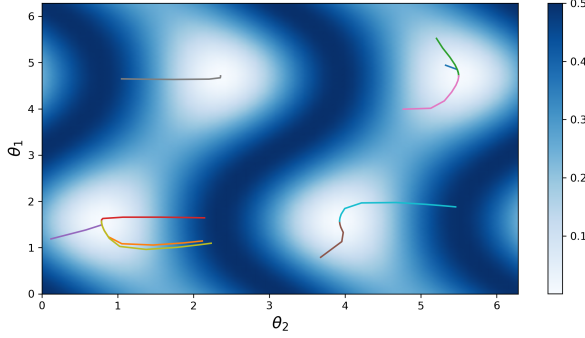


FIG. 9: Parameters of states for each step in space of all possible parameters for the case of a quantum simulator. The colors of the curves correspond to those in Fig. 8. The heatmap represents value of the cost function.

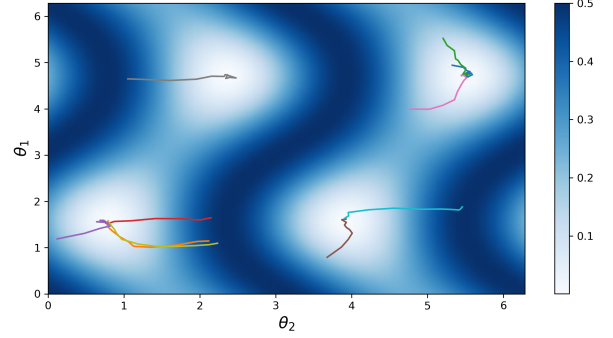


FIG. 12: Parameters of states for each step in space of all possible parameters for the case of Yorktown quantum processor. The colors of the curves correspond to those in Fig. 11. The heatmap represents values of the cost function.

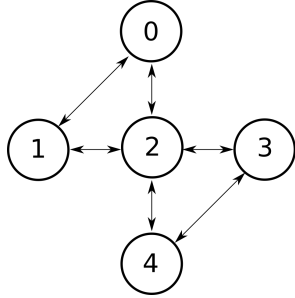


FIG. 10: Connectivity of qubits in the Yorktown processor.

of the optimization procedure.

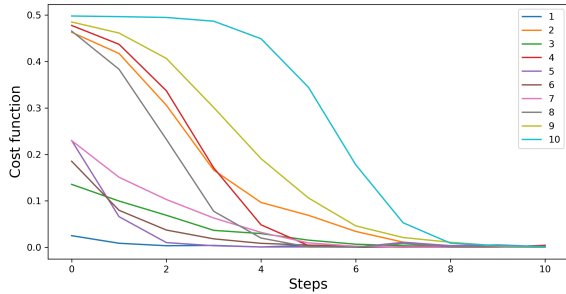


FIG. 11: Cost function during minimalization for 10 runs with randomly initialize parameters. Values compute on simulator based on parameters obtained on IBM Yorktown quantum computer.

Fig. 12 shows the cost function in the parameter space. In consequence of the applied optimization procedure the state, for which measured amplitudes are shown in Fig. 13, has been found. Without error correction methods and with automatic transpilation of circuit we obtained fidelity of the found state equal 0.9973 ± 0.0029 .

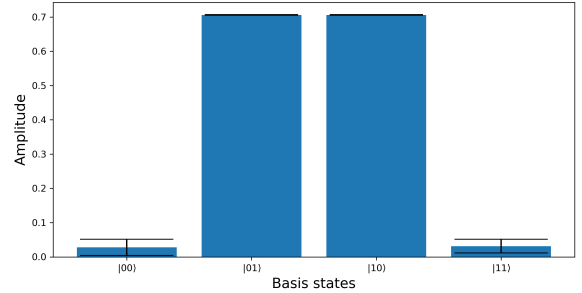


FIG. 13: Averaged amplitudes of the final state obtained from over the 10 runs. The RYCZ ansatz implies that the amplitudes are real valued. The error bars correspond to standard deviation.

VIII. THE $s = 2$ CASE

In this case, the constrain squared consists of more Pauli terms, which have to be evaluated independently

| No. | Fidelity | Cost |
|-----|----------|---------|
| 1. | 0.99825 | 0.00014 |
| 2. | 0.99831 | 0.00013 |
| 3. | 0.92892 | 0.00915 |
| 4. | 0.63477 | 0.00434 |
| 5. | 0.00383 | 0.01019 |
| 6. | 0.64508 | 0.00430 |
| 7. | 0.99777 | 0.00006 |
| 8. | 0.99825 | 0.00014 |
| 9. | 0.98189 | 0.00226 |
| 10. | 0.99825 | 0.00014 |

TABLE I: Fidelities of the obtained states and final values of the cost function corresponding to these states for 10 runs.

and then summed up:

$$\begin{aligned}
\hat{C}^2 = & \frac{1}{16} \left(P_n(\sigma_y, \sigma_y) \left(\frac{16}{3} - \frac{76}{3}\delta + 16\delta^2 \right) \right. \\
& + P_n(\sigma_z, \sigma_z) \left(\frac{34}{9} - 40\delta + 144\delta^2 \right) \\
& + P_n(\sigma_x, \sigma_x) \left(2 - \frac{4}{3}\delta + 16\delta^2 \right) \\
& + \mathbb{I}^{\otimes 4} \left(\frac{208}{9} - 144\delta + 384\delta^2 \right) \\
& + P_n(\sigma_x, \sigma_x, \sigma_y, \sigma_y) \\
& + P_n(\sigma_z, \sigma_z, \sigma_z, \sigma_z) \left(-\frac{2}{3}\delta + 8\delta^2 \right) \\
& + P_n(\sigma_y, \sigma_y, \sigma_z, \sigma_z) \left(\frac{5}{3} - \frac{38}{3}\delta + 8\delta^2 \right) \\
& \left. + P_n(\sigma_x, \sigma_x, \sigma_z, \sigma_z) \left(-\frac{2}{3}\delta + 8\delta^2 \right) \right). \quad (76)
\end{aligned}$$

Here, we use also the RYCZ ansatz but for 4 qubits, and with 2 layers, and 6 real parameters (see Fig. 14).

Fig. 15 shows the cost function in a function of steps of the optimization procedure employing simulator of a quantum computer.

In all cases (6 out of 10) when cost function decreases under 0.004 we obtain states with fidelity above 0.98, in cases (2 out of 10) with cost function slightly above 0.04 we obtain fidelity around 0.64. Interesting is case with high fidelity 0.93 but with cost function quite high 0.009, which means that even if we stuck in some local minimum we have chance to obtain state close to correct one. The obtained fidelities are collected in Tab. I.

In the case of $s = 2$ for $\delta = \frac{7}{18}$ the kernel of \hat{C} is degenerated, $\dim \ker \hat{C} = 3$. A linearly independent set of states spanning the kernel can be found using the method discussed in Sec. V. In Tab. II results of the Gram-Schmidt procedure for five runs are shown. In all case, there are three leading contributions and the fourth one is marginal. This provides evidence that the kernel space

| No. | Step 1. | Step 2. | Step 3. | Step 4. |
|-----|---------|---------|---------|---------|
| 1. | 1.0000 | 0.9998 | 0.0764 | 0.0006 |
| 2. | 1.0000 | 0.9038 | 0.6065 | 0.0002 |
| 3. | 1.0000 | 0.1097 | 0.4148 | 0.0040 |
| 4. | 1.0000 | 0.9984 | 0.0003 | 0.2669 |
| 5. | 1.0000 | 0.7227 | 0.0000 | 0.8264 |

TABLE II: Norms of states obtained in each step of the Gram-Schmidt procedure (before normalization of the states) for 5 runs of the optimization procedure for the case with $s = 2$ and $\delta = \frac{7}{18}$.

is three dimensional, in accordance to the theoretical expectations for the case with $\delta = \frac{7}{18}$. However, due to computational errors, the answer is not fully conclusive.

IX. COMPUTATIONAL COMPLEXITY

As we see the case $s = 2$ has many more terms to evaluate than the case $s = 1$. Consequently, in the large spin limit a problem of enormous number of terms may arise. To analyze the number of Pauli terms for arbitrary spin s , let us first notice that the number of different Pauli terms in operator P_n is given by the combinatorial factor:

$$\frac{n!}{n_x!n_y!n_z!(n-n_x-n_y-n_z)!}, \quad (77)$$

where n_k is number of Pauli operators σ^k and n is number of qubits. Using formula (53) for C^2 for arbitrary spin we obtain (for $n \geq 6$) number of Pauli terms, i.e. number of quantum circuits to evaluate is:

$$\begin{aligned}
& \frac{151}{720}n(n-1)(n-2)(n-3)(n-4)(n-5) \\
& + \frac{7}{8}n(n-1)(n-2)(n-3) + \frac{3}{2}n(n-1) \sim n^6, \quad (78)
\end{aligned}$$

which, fortunately, has polynomial computational complexity $\mathcal{O}(n^6)$. Here, symmetries of the constraint (which may slightly reduce the number of combinations) were not taken into account.

Another aspect of computational complexity of the method relates to the fact that in the proposed method a subspace of the total Hilbert space of the quantum register is used. For a register composed of n qubits, the Hilbert space has dimension 2^n . However, the constraint (with fixed spin s) subspace forms a $2s+1 = n+1$ dimensional subspace. The remaining $2^n - (n+1)$ states of the register are not used. This is unavoidably a waste of quantum resources, and the weak side of the approach. Please notice that the spin s scales linearly with the number of qubits. So, for instance with 16 qubits we can simulate only a system with spin $s = 8$.

The ideal situation would be to utilize the whole Hilbert space of the quantum register, so that $2s+1 = 2^n$. In such case, having $n = 16$ qubits allows to simulate with

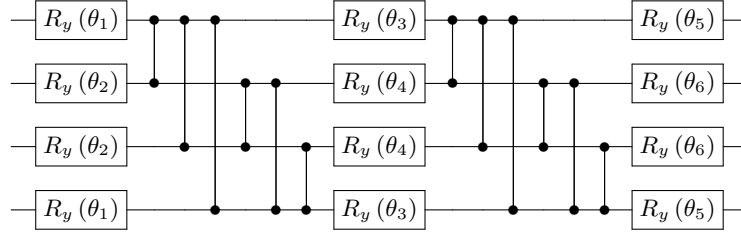
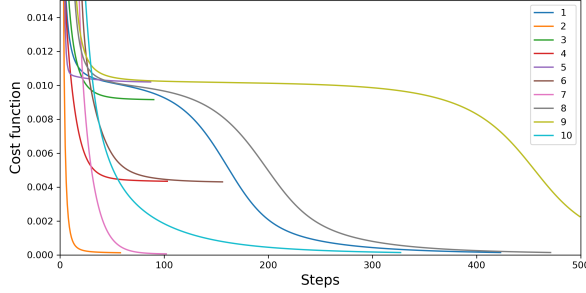


FIG. 14: Quantum circuit for the ansatz for spin 2.

FIG. 15: Cost function during minimalization for 10 runs with randomly initialize parameters. Here, the RY-CZ ansatz and $\delta = 1/2$ have been used.

$s \sim 3 \cdot 10^4$. Finding a method of representing spin operators and constraints in this case is an open problem, which will be addressed elsewhere.

The advantage of the method presented here becomes, however, sound while systems with sufficiently high numbers (m) of the classical degrees of freedom are considered. Then, assuming that for every degree of freedom the spin representation is s , the dimension of the Hilbert space of the composite system is $(2s + 1)^m$. Every spin consumes $n = 2s$ qubits of the quantum register, so in total $nm = 2sm$ qubits are needed. So, smaller the s less of the quantum resources are wasted, i.e. $2^{2sm} - (2s + 1)^m$. In the limiting case of $s = 1/2$, all the quantum resources are utilized $2^{2 \cdot \frac{1}{2} m} - (2 \cdot \frac{1}{2} + 1)^m = 0$. In this range, application of quantum methods prognoses to be advantageous over the classical method, since the amount of utilized computational resources grows exponentially with m .

X. SUMMARY

In this article we have introduced and tested a method of solving of Wheeler-DeWitt equation employing variational quantum methods. For a single constraint C , having m classical degrees of freedom, the methods consists of the following main steps:

1. Replace the kinematical phase space $\Gamma = \mathbb{R}^{2m}$ with $\Gamma = \mathbb{S}^{2m}$.
2. Express the constraint C in terms of spin variables

$C(\vec{S}_1, \dots, \vec{S}_m)$. This can be done by applying the replacement:

$$p \rightarrow \frac{S_y}{R_2}, \quad q \rightarrow -\frac{S_z}{R_1},$$

where $R_1 R_2 = S$, for every canonical pair (q_i, p_i) .

3. Perform canonical quantization and symmetrization of the constraint, obtaining $\hat{C}(\vec{S}_1, \dots, \vec{S}_m)$. Fix a particular representation s for the spins.
4. Represent the spin operators in terms of qubits, employing the formula:

$$\hat{S}_i = \frac{1}{2} \sum_{j=1}^n \mathbb{I}^1 \otimes \dots \otimes \mathbb{I}^{j-1} \otimes \hat{\sigma}_i^j \otimes \mathbb{I}^{j+1} \otimes \dots \otimes \mathbb{I}^n,$$

where $n = 2s$.

5. Apply the the VQE method with the cost function:

$$c(\alpha) = \frac{a}{\max |\lambda_i|^2} \langle \psi(\alpha) | \hat{C}^\dagger \hat{C} | \psi(\alpha) \rangle + b \left(1 - \frac{\langle \hat{S}^2 \rangle}{s(s+1)} \right),$$

where $a + b = 1$, and $a, b \in (0, 1)$ (e.g. $a = \frac{1}{2} = b$).

6. Explore degeneracy of the kernel space by either adding terms $|\langle \psi_i | \psi(\alpha) \rangle|$ to the cost function or by applying the Gramm-Schmidt procedure.
7. Study the large s limit to recover results for the case of the flat (affine) phase space.

The procedure utilizes compactification of the system's phase space for the purpose of making its Hilbert space finite. The dimension of the Hilbert space is controlled by a single parameter s , which labels irreducible representations of the $SU(2)$ group. The flat phase space case is recovered in the large spin s limit. In the article, the procedure has been tested on the example of a de Sitter cosmological model, which has a single classical degree of freedom (the scale factor) and consequently two-dimensional phase space. In the quantum case, the kinematics is described by the spin operators \vec{S} . Quantum constraint of the system has been expressed in terms

of the action qubits of the quantum register for an arbitrary spin s . This allowed to perform the VQE method and extract physical states.

As an example, the procedure has been executed for $s = 1$ and $s = 2$. In the case of $s = 1$ the quantum circuits were evaluated on both simulator of the quantum computer and superconducting quantum computer Yorktown. In case $s = 2$ the computations have been performed on a simulator only due to high quantum errors. Both the case of non-degenerate and degenerate kernel was explored, confirming correctness of the method.

As it has been emphasized, the method introduced do not provide advantage over classical computations for the case of a single degree of freedom (relevant in homogeneous and isotropic cosmology). However, the advantage is expected while a large number of quantum-gravitational degrees of freedom is considered. Investigation of such a case will be a subject of our further studies.

ACKNOWLEDGMENTS

The research has been supported by the Sonata Bis Grant No. DEC-2017/26/E/ST2/00763 of the National Science Centre Poland. This research was funded by the Priority Research Area Digiworld under the program Excellence Initiative – Research University at the Jagiellonian University in Kraków. Furthermore, this publication was made possible through the support of the ID# 61466 grant from the John Templeton Foundation, as part of the “The Quantum Information Structure of Spacetime (QISS)” Project (qiss.fr). The opinions expressed in this publication are those of the authors and do not necessarily reflect the views of the John Templeton Foundation.

APPENDIX A

RYCZ ansatz consists of R_y (RY):

$$R_y(\theta) = \exp\left(-i\frac{\theta}{2}\sigma_y\right) = \begin{pmatrix} \cos\frac{\theta}{2} & -\sin\frac{\theta}{2} \\ \sin\frac{\theta}{2} & \cos\frac{\theta}{2} \end{pmatrix}, \quad (79)$$

and controlled- σ_z (CZ) gates.

We apply gates $R_y(\theta_i)$, parameterized by different parameters θ_i , on every qubit and then we apply CZ gates on all pairs of qubits (Fig. 16) or only on some pairs (Fig. 17). This block of gates can be repeated many times (Fig. 18).

This ansatz generates states with real coefficients, but since \hat{C} is self-adjoint, we can always choose eigenvectors to be real. Let $|v\rangle$ be eigenvector with complex coefficients for λ eigenvalue (which is real):

$$\hat{C}|v\rangle = \lambda|v\rangle. \quad (80)$$

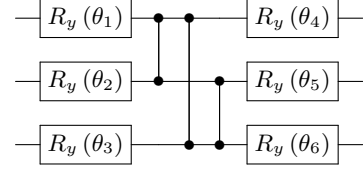


FIG. 16: Quantum circuit for the RY ansatz with full entanglement, and depth = 1.

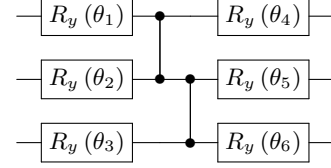


FIG. 17: Quantum circuit for the RY ansatz with linear entanglement, and depth = 1.

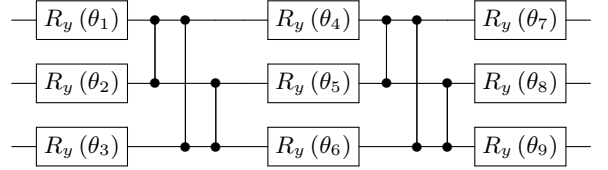


FIG. 18: Quantum circuit for the RY ansatz with full entanglement, and depth = 2.

Then $|\bar{v}\rangle = |v\rangle^*$ is also eigenvector for the same eigenvalue:

$$\hat{C}|\bar{v}\rangle = \lambda|\bar{v}\rangle. \quad (81)$$

In consequence, we can take linear combination of these vectors:

$$|a\rangle = \frac{1}{2}(|v\rangle + |\bar{v}\rangle), \quad (82)$$

$$|b\rangle = \frac{1}{2i}(|v\rangle - |\bar{v}\rangle), \quad (83)$$

which are real eigenvectors to the eigenvalue λ .

Ansatz from Sec. VII can be expressed as RYCZ ansatz by:

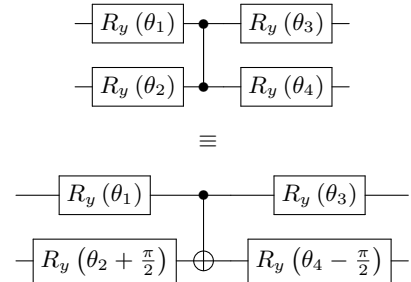


FIG. 19: Quantum circuit for the RYCZ ansatz.

-
- [1] J. B. Hartle and S. W. Hawking, *Phys. Rev. D* **28**, 2960 (1983).
- [2] A. Vilenkin, *Phys. Rev. D* **30**, 509(R) (1984).
- [3] A. Ashtekar, J. Lewandowski, D. Marolf, J. Mourao and T. Thiemann, *J. Math. Phys.* **36** (1995), 6456-6493 [arXiv:gr-qc/9504018 [gr-qc]].
- [4] T. Thiemann, *Class. Quant. Grav.* **23** (2006), 1163-1180 [arXiv:gr-qc/0411031 [gr-qc]].
- [5] J. Mielczarek and W. Piechocki, *Class. Quant. Grav.* **29** (2012), 065022 [arXiv:1107.4686 [gr-qc]].
- [6] J. Mielczarek, *Front. Astron. Space Sci.* **8** (2021), 95
- [7] A. Peruzzo, J. McClean, P. Shadbolt, *et al.*, *Nature Communications* **5**, 4213 (2014).
- [8] A. Kandala, *et al.*, *Nature* **549**, 242 (2017).
- [9] Y. Cao, *et al.*, *Chemical Reviews* **119** (19), 10856 (2019).
- [10] <https://pennylane.ai/>
- [11] <https://qiskit.org/>
- [12] <https://quantum-computing.ibm.com/>
- [13] J. Mielczarek and T. Trzeńniewski, *Phys. Lett. B* **759** (2016), 424-429 [arXiv:1601.04515 [hep-th]].
- [14] N. Bao, S. M. Carroll and A. Singh, *Int. J. Mod. Phys. D* **26** (2017) no.12, 1743013 [arXiv:1704.00066 [hep-th]].
- [15] C. Rovelli and F. Vidotto, *Phys. Rev. D* **91** (2015) no.8, 084037 [arXiv:1502.00278 [gr-qc]].
- [16] D. Artigas, J. Mielczarek and C. Rovelli, *Phys. Rev. D* **100** (2019) no.4, 043533 [arXiv:1904.11338 [gr-qc]].
- [17] D. Artigas, J. Bilski, S. Crowe, J. Mielczarek and T. Trzeńniewski, *Phys. Rev. D* **102** (2020) no.12, 125029 [arXiv:2008.01729 [hep-th]].
- [18] J. Mielczarek, *Universe* **5** (2019) no.8, 179 [arXiv:1810.07100 [gr-qc]].
- [19] M. J. D. Powell, 1994. *Advances in Optimization and Numerical Analysis*, eds. S. Gomez and J-P Hennart, Kluwer Academic (Dordrecht), 51-67.
- [20] D. Kingma, J. Ba. Published as a conference paper at the 3rd International Conference for Learning Representations, San Diego, 2015, [arXiv:1412.6980 [cs.LG]].
- [21] M. Schuld, V. Bergholm, C. Gogolin, J. Izaac, and N. Kilorian *Phys. Rev. A* **99**, 032331 (2019).